Int J Mech Mater Des (2017) 13:243–252
DOI 10.1007/s10999-015-9330-1

Adjoint design sensitivity analysis of constant temperature molecular dynamics

Hong-Lae Jang · Seonho Cho

Received: 30 October 2015 / Accepted: 18 November 2015 / Published online: 26 November 2015

Abstract In this research, we proposed an efficient design sensitivity analysis (DSA) method for constant temperature molecular dynamics (MD). A Nose–Hoover thermostat is utilized to represent the possible state of a system that is in thermal equilibrium using a heat bath to maintain temperature constant. The design sensitivity of general performance measures is derived using an adjoint variable method. Since the adjoint system is path-dependent and derived in the form of a terminal value problem, the path of original MD analysis should be kept to be used with in the adjoint sensitivity computation. The time reversibility of the MD system with Nose–Hoover thermostat is investigated. The accuracy and efficiency of the developed adjoint DSA method are verified through demonstrative numerical examples.

Keywords Molecular dynamics · Adjoint variable method · Transient dynamic sensitivity · Nose–Hoover thermostat · Time reversibility

H.-L. Jang · S. Cho (✉)
National Creative Research Initiatives (NCRI) Center for Isogeometric Optimal Design, Department of Naval Architecture and Ocean Engineering, Seoul National University, 1 Gwanak-ro, Gwanak-gu, Seoul 151-744, Korea
e-mail: secho@snu.ac.kr

H.-L. Jang
e-mail: perr83@snu.ac.kr

1 Introduction

Within the past decades the nanotechnology has received considerable attention as more and more practical applications of nanomaterials are emerging in the field of physics, chemistry, and biomedicine. The MD simulation is one of the most popular tools to study the mechanical behaviors of nanomaterials in atomistic level. In the MD simulation, the Hamiltons equations are solved for sampling the microcanonical constant energy distribution. However, it is convenient to keep the temperature constant in physical experiments. Therefore performing constant temperature MD simulation is of great importance for the investigation of physical, chemical, and biological problems.

Several approaches have been proposed for this purpose. Since the temperature is related to the kinetic energy, the velocities of atoms in the system must be rescaled in order to maintain the temperature at desired value. One crude way is direct rescaling of the velocities at each time step after a certain number of time steps. However, this direct velocity rescaling does not sample the phase space in a proper way as prescribed for a canonical ensemble since the condition of constant temperature is not equivalent to the condition that the kinetic energy per atom is constant from a statistical mechanical point of view (Frenkel and Smit 2001). Andersen (Andersen 1980) proposed a constant temperature MD simulation method which is a hybrid of MD and Monte Carlo (MC) methods since the velocities of the atoms are changed by

stochastic collisions to induce the Boltzmann distribution. The stochastic collisions introduce drastic changes to the dynamics in an unrealistic way and it also lacks a well-defined conserved quantity. In the Berendsen method (Berendsen et al. 1984), the velocities of atoms are rescaled more gradually than the Anderson method. The thermostat suppresses fluctuations of the kinetic energy of system and therefore cannot generate a correct canonical ensemble rigorously. Based on the extended Lagrangian approach introduced by Andersen (Andersen 1980), Nose introduced an extended Hamiltonian which consists of additional degrees of freedom of the heat bath that acts as a time scaling factor (Nosé 1984a, b). Noses method is simplified by Hoover (Hoover 1985) by introducing a thermodynamic friction coefficient. Hoovers formulation of Noses method is so-called the Nose–Hoover thermostat. If an ergodic dynamic behavior is assumed, the correct canonical distribution can be obtained by utilizing the Nose–Hoover thermostat. However, for small or stiff systems, the Nose–Hoover dynamics is not ergodic (Hoover 1985; Tuckerman et al. 2001). Martyna and co-workers (Martyna et al. 1992; Tobias et al. 1993) proposed a Nose–Hoover chain method to fix these problems. However, for the system that is large enough to be sufficiently chaotic, the ergodicity is guaranteed so that the performance of Nose–Hoover thermostat is usually satisfactory (Frenkel and Smit 2001). The generalized Langevin equation (GLE) proposed by Adelman and Doll (Adelman and Doll 1974, 1976) is also used for the constant temperature MD simulation (Ceriotti et al. 2009; Evstigneev and Reimann 2010). The random and frictional forces in the GLE are balanced to maintain the desired system temperature (Hu and Sinnott 2004; Kim et al. 2013b).

In the viewpoint of design aspects, the temperature is one of significant design variables that can be controlled to a certain value in both simulations and experiments. The temperature effect of various properties of nanomaterials such as nanowires (Koh and Lee 2006; Wu 2006), nanoparticles (Shibuta and Suzuki 2008) have been reported and discussed by using MD simulations. However, the way to study temperature effect on nanomaterial properties relies on trial and error. With the help of design sensitivity analysis (DSA), one can quantify the effect of parameters such as temperature on the results from simulations as well as experiments efficiently. Also, the gradient of simulation parameters can be changed when the operation temperature varies. Therefore, an accurate and efficient DSA method is required considering the NVT ensemble. Molecular dynamics is a typical transient dynamic problem but there are few literature regarding the DSA methods for transient dynamics. The AVM for transient dynamics was well established in the reference (Choi and Kim 2006) and the corresponding adjoint system turned out to be a terminal value problem. Hsieh and Arora (Hsieh and Arora 1984) developed DSA methods using both DDM and AVM for dynamic problems with pointwise constraints. Tsay and Arora (1990) derived nonlinear DSA for path-dependent problems using total Lagrangian formulation considering geometrical and material nonlinearities. However, they follow all the history of solution procedure for the DSA because the dynamic equations for both original responses and design sensitivities are path-dependent (Cho and Choi 2000). This makes it difficult to extend DSA methods to the molecular dynamics since the adjoint system that corresponds to MD simulations is usually a path-dependent problems. Adjoint DSA method for the MD system where the number of atoms N, volume V and energy E is fixed (NVE ensemble) is already proposed (Jang et al. 2014). Since the equation of motion for the NVE ensemble is conservative, when the performance measure is only dependent on the state at terminal time and the internal force term is linear with respect to the displacement due to the harmonic approximation of the inter-atomic potential, the adjoint equation of motion can be independently solved from the original system. In that case, there is an advantage of saving the computational storage to keep the original response history (Kim et al. 2013a, b). In the case of non-linear internal forces, however, the adjoint equations depend on the path of original response and thus the tangent stiffness in the adjoint systems changes with each time. In this case, the adjoint problem is history-dependent, which means that we must follow all the history of response analysis for solving the problem. In this paper, we developed an adjoint DSA method for the constant temperature MD simulations. To obtain the continuous trajectory of a system having constant number N of atoms, volume V, and temperature T (NVT ensemble), the Nose–Hoover thermostat is utilized. In contrast with the adjoint system of NVE ensemble, the adjoint system of NVT ensemble is inherently path-dependent due to the additional

degrees of freedom corresponding to the heat bath which acts as a damping term.

The remainder of this paper is organized as follows. In Sect. 2, we briefly review the Nose–Hoover thermostat. In Sect. 3, we discuss the DSA of constant temperature MD, where both the DDM and the AVM are considered. Due to the effect of the external heat bath, the equation of motion for Nose–Hoover thermostat is a path-dependent problem so that the kinematics of atoms and thermodynamic friction coefficients must be kept at each time step for the AVM. Also, the design sensitivity of extended Hamiltonian which is conserved quantity is discussed. In Sect. 4, we present demonstrative numerical examples, where the accuracy and efficiency of the derived adjoint sensitivity are verified. For the design parameterization of instantaneously desired temperature, a rectangular pulse function is introduced to interpolate the temperature as a function of time.

2 Review of Nose–Hoover thermostat

To perform MD simulations on a system where the number of particles N, the volume V, and the temperature T are fixed, we consider a physical system that contacts with a heat bath. Hamiltonian for the *extended system* can be written, in terms of the extended variables, as

$$H(\tilde{p}, q, \tilde{p}_s, s) = \sum_{i=1}^{3N} \frac{\tilde{p}_i^2}{2m_i s^2} + \frac{\tilde{p}_s^2}{2Q} + V_{pot}(q) + z \ln s, \tag{1}$$

where q, $\tilde{p}$, and V_{pot} are the atomic position, the momenta conjugate to q, and potential energy function respectively. s, $\tilde{p}_s$, and Q denote the additional degrees of freedom for the heat bath, the momentum conjugate to s, and an effective mass associated to s. z is a factor for sampling a canonical distribution. The tilde denotes the extended variables corresponding to the scaled time τ.

The equation of motion of the extended system variables are found to be the followings.

$$\frac{d\tilde{p}_i}{d\tau} = F_i, \tag{2}$$

$$\frac{dq_i}{d\tau} = \frac{\tilde{p}_i}{m_i s^2}, \tag{3}$$

$$\frac{d\tilde{p}_s}{d\tau} = \sum_{i=1}^{3N} \frac{\tilde{p}_i^2}{m_i s^3} - z\frac{1}{s}, \tag{4}$$

and

$$\frac{ds}{d\tau} = \frac{\tilde{p}_s}{Q}. \tag{5}$$

It can be considered that the real (physical) time t is scaled to the scale time τ in the extended system according to

$$d\tau = sdt. \tag{6}$$

If we sample the canonical distribution or calculate the ensemble average with the extended variable τ, the sampling is done at integer multiples of the extended time step $\Delta\tau$ that are not constant. Therefore, for the sampling at equal intervals in physical time, it could be convenient to do the integrations in terms of the *physical system* variables by means of the transformations $p_i = \tilde{p}_i/s$ and Eq. (6). Using the transformations, we can come up with the equation of motion for physical system variables and heat bath variables,

$$\dot{p}_i = F_i - p_i\frac{\dot{s}}{s}, \tag{7}$$

$$\dot{q}_i = \frac{p_i}{m_i}, \tag{8}$$

$$\dot{p}_s = \sum_{i=1}^{3N} \frac{p_i^2}{m_i} - z, \tag{9}$$

and

$$\dot{s} = s\frac{p_s}{Q}. \tag{10}$$

We can obtain the second order Lagrangian equation of motion in terms of physical variables which most often are used in MD simulations by combining the first order equations of motion. By introducing the friction coefficient $\zeta = \dot{s}/s$ proposed by Hoover (Hoover 1985), the equations of motion are obtained by

$$\ddot{q}_i = \frac{F_i}{m_i} - \dot{q}_i\zeta \tag{11}$$

and

$$\dot{\zeta} = \frac{1}{Q}\left(\sum_{i=1}^{3N} m_i\dot{q}_i^2 - z\right). \tag{12}$$

The factor z is determined to recover the canonical sampling

$$z = 3Nk_BT. \tag{13}$$

Notice that the number of atoms N is used in Eq. (13) since the Eqs. (11) and (12) are written in physical variable formulation.

3 Design sensitivity analysis of Nose–Hoover thermostat

3.1 Adjoint variable method

A general performance measure ψ of Nose–Hoover thermostat can be defined including both terminal time value and time history quantity as

$$\psi = g(\mathbf{b}, \zeta, \mathbf{q}, \dot{\mathbf{q}})|_{t=t_T} + \int_0^{t_T} h(\mathbf{b}, \zeta, \mathbf{q}, \dot{\mathbf{q}})dt. \tag{14}$$

Taking the first order variation of Eq. (14) with respect to design $\mathbf{b}$ and integrating by parts lead to

$$\begin{aligned}\psi' = &\left(\frac{\partial g}{\partial \mathbf{b}}\delta\mathbf{b} + \frac{\partial g}{\partial \zeta}\zeta' + \left(\frac{\partial g}{\partial \mathbf{q}} + \frac{\partial h}{\partial \dot{\mathbf{q}}}\right)\mathbf{q}' + \frac{\partial g}{\partial \dot{\mathbf{q}}}\dot{\mathbf{q}}'\right)\Bigg|_{t=t_T} \\ &+ \int_0^{t_T}\left(\frac{\partial h}{\partial \mathbf{b}}\delta\mathbf{b} + \frac{\partial h}{\partial \zeta}\zeta' + \left(\frac{\partial h}{\partial \mathbf{q}} - \frac{d}{dt}\frac{\partial h}{\partial \dot{\mathbf{q}}}\right)\mathbf{q}'\right)dt.\end{aligned} \tag{15}$$

Equations of motion for Nose–Hoover thermostat can be re-written, in a matrix-vector form for convenience, as

$$\mathbf{m}_A\ddot{\mathbf{q}}(t) = \mathbf{f} - \zeta(t)\mathbf{m}_A\dot{\mathbf{q}}(t), \tag{16}$$

$$Q\dot{\zeta}(t) = \dot{\mathbf{q}}(t)^T\mathbf{m}_A\dot{\mathbf{q}}(t) - z. \tag{17}$$

Two adjoint variables $\lambda(t)$ and $\xi(t)$ are introduced. Note that $\lambda(t)$ is a vector function whereas $\xi(t)$ is a scalar function related to the thermostat variable. Multiplying the adjoint variables and integrating with respect to time, we have

$$\begin{aligned}&\int_0^{t_T}\lambda^T(\mathbf{m}_A(\mathbf{b})\ddot{\mathbf{q}} - \mathbf{f}(\mathbf{b}, \mathbf{q}) + \mathbf{m}_A(\mathbf{b})\zeta\dot{\mathbf{q}})dt \\ &+ \int_0^{t_T}\xi\Big(Q(\mathbf{b})\dot{\zeta} - \dot{\mathbf{q}}^T\mathbf{m}_A(\mathbf{b})\dot{\mathbf{q}} + z(\mathbf{b})\Big)dt = 0.\end{aligned} \tag{18}$$

Assuming that the Lagrange multipliers are independent of design, taking first order variation of Eq. (18) and integrating by parts yields

$$\begin{aligned}&\Big(\lambda^T\mathbf{m}_A\dot{\mathbf{q}}' + \Big(\lambda^T\zeta\mathbf{m}_A - \dot{\lambda}^T\mathbf{m}_A - 2\xi\dot{\mathbf{q}}^T\mathbf{m}_A\Big)\mathbf{q}' + \xi Q\zeta'\Big)\Big|_{t=t_T} \\ &+ \int_0^{t_T}\Big(\ddot{\lambda}^T\mathbf{m}_A - \lambda^T\frac{\partial \mathbf{f}}{\partial \mathbf{q}} - \dot{\lambda}^T\zeta\mathbf{m}_A - \lambda^T\dot{\zeta}\mathbf{m}_A \\ &+ 2\xi\ddot{\mathbf{q}}^T\mathbf{m}_A + 2\dot{\xi}\dot{\mathbf{q}}^T\mathbf{m}_A\Big)\mathbf{q}'dt \\ &+ \int_0^{t_T}\Big(\lambda^T\mathbf{m}_A\dot{\mathbf{q}} - \dot{\xi}Q\Big)\zeta'dt \\ &= -\int_0^{t_T}\left\{\lambda^T\left(\frac{\partial \mathbf{m}_A}{\partial \mathbf{b}}\ddot{\mathbf{q}} - \frac{\partial \mathbf{f}}{\partial \mathbf{b}} + \frac{\partial \mathbf{m}_A}{\partial \mathbf{b}}\zeta\dot{\mathbf{q}}\right)\right. \\ &\quad\left. + \xi\left(\frac{\partial z}{\partial \mathbf{b}} + \frac{\partial Q}{\partial \mathbf{b}}\dot{\zeta} - \dot{\mathbf{q}}^T\frac{\partial \mathbf{m}_A}{\partial \mathbf{b}}\dot{\mathbf{q}}\right)\right\}\delta\mathbf{b}dt.\end{aligned} \tag{19}$$

Matching the resulting identity of Eqs. (19) with (15), we can obtain the following adjoint system and the corresponding terminal conditions for the MD systems of NVT ensemble.

$$\begin{aligned}\ddot{\lambda} = &\zeta\dot{\lambda} + \mathbf{m}_A^{-1}\frac{\partial \mathbf{f}}{\partial \mathbf{q}}\lambda + \dot{\zeta}\lambda - 2\xi\ddot{\mathbf{q}} - 2\dot{\xi}\dot{\mathbf{q}} \\ &+ \mathbf{m}_A^{-1}\left(\frac{\partial h}{\partial \mathbf{q}} - \frac{d}{dt}\frac{\partial h}{\partial \dot{\mathbf{q}}}\right)^T,\end{aligned} \tag{20}$$

$$\dot{\xi} = \frac{1}{Q}\left(\lambda^T\mathbf{m}_A\dot{\mathbf{q}} - \frac{\partial h}{\partial \zeta}\right), \tag{21}$$

$$\xi(t_T) = \frac{1}{Q}\frac{\partial g}{\partial \zeta}, \tag{22}$$

$$\lambda(t_T) = \mathbf{m}_A^{-1}\left(\frac{\partial g}{\partial \dot{\mathbf{q}}}\right)^T, \tag{23}$$

and

$$\dot{\lambda}(t_T) = \mathbf{m}_A^{-1}\left\{\zeta\left(\frac{\partial g}{\partial \dot{\mathbf{q}}}\right)^T - \left(\frac{\partial g}{\partial \mathbf{q}} + \frac{\partial h}{\partial \dot{\mathbf{q}}}\right)^T\right\} - \frac{2}{Q}\left(\frac{\partial g}{\partial \zeta}\right)\dot{\mathbf{q}}. \tag{24}$$

Thus, the adjoint design sensitivity can be obtained from the original and adjoint responses,

$$\psi' = \frac{\partial g}{\partial \mathbf{b}}\delta\mathbf{b}\bigg|_{t=t_T} + \int_0^{t_T} \frac{\partial h}{\partial \mathbf{b}}\delta\mathbf{b}dt - \int_0^{t_T} \left\{ \lambda^T \left(\frac{\partial \mathbf{m}_A}{\partial \mathbf{b}}(\ddot{\mathbf{q}} + \zeta\dot{\mathbf{q}}) - \frac{\partial \mathbf{f}}{\partial \mathbf{b}} \right) + \xi \left(\frac{\partial z}{\partial \mathbf{b}} + \frac{\partial Q}{\partial \mathbf{b}}\dot{\zeta} - \dot{\mathbf{q}}^T \frac{\partial \mathbf{m}_A}{\partial \mathbf{b}}\dot{\mathbf{q}} \right) \right\} \delta\mathbf{b}dt. \tag{25}$$

3.2 Time reversibility of adjoint systems: NVE and NVT ensembles

For transient dynamic problems, the corresponding adjoint equation is usually a terminal value problem as derived in Eqs. (20) and (21). Therefore, the initial conditions of adjoint responses can be recovered due to the time reversibility of the system. A reversible system is defined as any second-order system that is invariant under the reversed time and velocity. Only the initial conditions, not the equations, can differ in the *reversed flow* of the reversible system (Jang et al. 2014; Lamb and Roberts 1998; Strogatz 1994). By definition, the constant temperature MD utilizing Nose–Hoover thermostat is time-irreversible in theory due to the velocity-dependent force term in Eq. (11). To investigate the characteristics of adjoint system corresponding to the NVT ensemble, we consider a simple 1-D harmonic oscillator which is the same as the Hoovers problem (Hoover 1985),

$$\ddot{q} = -\frac{k}{m}q - \zeta\dot{q}, \tag{26}$$

$$\dot{\zeta} = \frac{m}{Q}\dot{q}^2 - \frac{z}{Q}, \tag{27}$$

where the parameters all taken to be unity, i.e. $m = 1$, $k = 1$, $Q = 1$, and $z = 1$. The initial conditions are set to $q(0) = \dot{q}(0) = 1$, $\zeta(0) = 1$ and the terminal time is $t_T = 100,000\delta t$, where $\delta t = 10^{-3}$. A half-step leap-frog scheme is utilized to integrate the dynamic system. When the performance measure is taken as the displacement at terminal time, $\psi = q(t_T)$, the resulting phase trajectory of adjoint system is shown in the Fig. 1a. Since the adjoint system is time irreversible, the resulting phase trajectory of the adjoint response shows chaotic behavior and there exists so many intersections through the trajectory. Therefore, only with the availability of whole time history of the original response in MD simulation stage enables us to solve the adjoint terminal value problem. In our previous research, we already investigated the time reversibility of response, sensitivity, and adjoint response of MD in the NVE ensemble (Jang et al. 2014). The phase trajectory of adjoint system corresponding to the NVE ensemble is shown in Fig. 1b. All the setting of the problem is the same as in the NVT case, but the thermostat is not considered in this problem to sample the NVE ensemble. Compared with

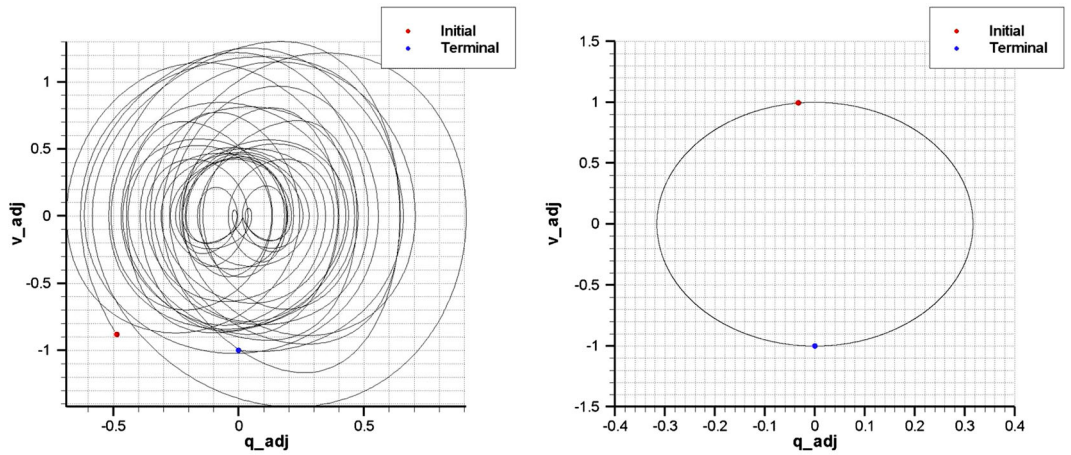

(a) Adjoint system for NVT ensemble **(b)** Adjoint system for NVE ensemble

Fig. 1 Phase trajectories of adjoint systems corresponding to **a** NVT and **b** NVE ensembles. In each phase trajectory, the *blue dots* denote the derived terminal conditions for adjoint responses and *red ones* denote the resulting initial conditions

Fig. 1a, b of the NVE adjoint system shows the characteristic of time reversible system which exhibits closed orbits and symmetry about the axis of adjoint displacement q_{adj}. Unlike the adjoint system of NVT ensemble, that of NVE ensemble is identical to the original system except initial conditions and thus can be solved from the terminal conditions independently where the potential function is harmonic. However, the adjoint system of NVT ensemble cannot be solved from the terminal conditions independently since the MD system in NVT ensemble is inherently time irreversible.

4 Numerical examples

To verify the accuracy and efficiency of the developed adjoint DSA method, an MD simulation for a tensile test of Cu nanowires is considered. A *3.615 nm*-long Cu nanowire is constructed by $5 \times 5 \times 10$ unit cells as shown in the Fig. 2 and the total number of atoms is 1270. The Embedded Atom Method (EAM) (Daw et al. 1993) is utilized to consider the bond between Cu atoms. The nanowire is at first thermally equilibrated at desired temperature for $5ps$ of 5,000 time steps using a Nose–Hoover thermostat while the Cu atoms in each end layer are fixed. The time step size for time integration is $\Delta t = 1fs$ and a half-step leap-frog scheme is utilized for the time integration. Periodic boundary conditions are not considered in any stage of the simulations and the DSA. After thermal equilibration, a tensile loading of constant strain rate is applied to the end layers. The strain rate is set to $\dot{\varepsilon} = 3 \times 10^{10} s^{-1}$. Engineering strain is defined as $\varepsilon_{zz} = (l_z - l_{z0})/l_{z0}$, where l_z is the current wire length in z direction and l_{z0} is the initial wire length. A yield strain is defined as the strain at which the maximum tensile stress occurs. The localized axial stress for atom i was calculated using the virial theorem, which has the form of (Koh and Lee 2006; Horstemeyer et al. 2001)

$$\eta^i_{zz}(\varepsilon) = \frac{1}{\Omega^i}\left(\frac{1}{2}\sum_{j=1, j\neq i}^{N} F^{ij}_z(\varepsilon) r^{ij}_z(\varepsilon)\right), \tag{28}$$

where F^{ij}_z refers to the [001] component of the interatomic force between atoms i and j. $r^{ij}_z = \left|x^i_z - x^j_z\right|$ is the interatomic distance in the [001] direction of the pair. Ω^i denotes the volume of atom i, which was assumed as a hard sphere in a closely packed un-deformed crystal structure. The axial stress on the nanowire is taken as the mean of the local stresses on all atoms as,

$$\sigma_{zz}(\varepsilon) = \frac{1}{N}\sum_{i=1}^{N} \eta^i_{zz}(\varepsilon). \tag{29}$$

The resulting yield strain and stress with respect to the various desired temperature are listed in Table 1. The recorded stress-strain curve is also presented in Fig. 3. When the temperature increases, the yield stress value is decreases as reported in literature (Koh and Lee 2006).

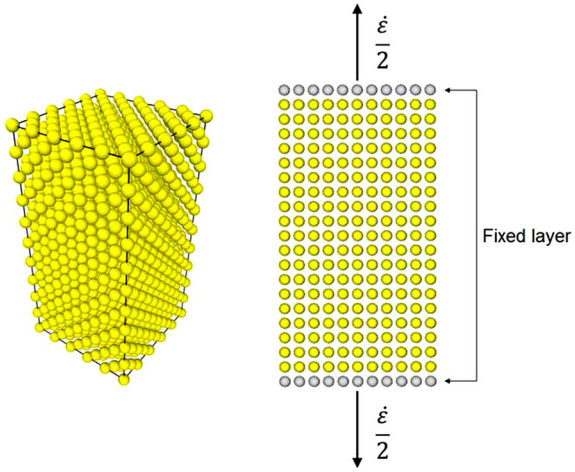

Fig. 2 Geometry of FCC metallic nanowire constructed by $5 \times 5 \times 10$ unit cells

4.1 Temperature sensitivity on Youngs modulus of nanowires

We performed the DSA to investigate the temperature effect on the Youngs modulus of Cu nanowires. The design variable is operation temperature T during the tensile loading which is design parameterized as $T = T_0(1 + b)$. Performance measure is the Youngs

Table 1 Yield stress and strain at different temperatures

Temperature	100 K	300 K	500 K
ε_Y	9.92E-02	9.93E-02	8.47E-02
σ_Y	10.34856	8.475221	6.798572

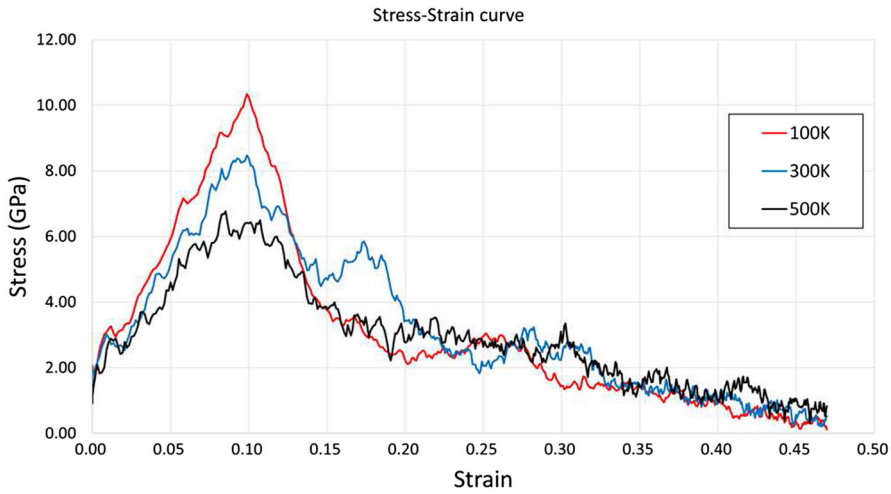

Fig. 3 Temperature effects on stress-strain curve of Cu nanowire

modulus of the copper nanowire obtained from the slope of linear regression line of stress-strain curve in the elasticity region. The Youngs modulus as the slope of the linear regression line can be written as

$$\psi = \frac{(t_2 - t_1)\int_{t_1}^{t_2} \varepsilon(t,\mathbf{b})\sigma(t,\mathbf{b},\mathbf{q})dt - \int_{t_1}^{t_2} \varepsilon(t,\mathbf{b})dt \int_{t_1}^{t_2} \sigma(t,\mathbf{b},\mathbf{q})dt}{(t_2 - t_1)\int_{t_1}^{t_2} \varepsilon^2(t,\mathbf{b})dt - \left(\int_{t_1}^{t_2} \varepsilon(t,\mathbf{b})dt\right)^2}, \tag{30}$$

where ε is the strain induced by the tensile loading, σ is the stress given as Eq. (29). t_1 and t_2 denote the time intervals where the linear regression analysis is performed. The time interval for calculating the Youngs modulus is between $t_1 = 5,500\Delta t$ and $t_2 = 9,000\Delta t$.Varying the strain-rate, we investigated the design sensitivity of temperature to the Youngs modulus by utilizing the developed adjoint DSA method. When decreasing the strain-rate, the required time for the yielding of nanowires becomes longer. The terminal times required for strain-rates of 3×10^{10}, 1.5×10^{10}, 6×10^{9}, and 3×10^{9} are 9000, 11000, 18000, and 25000 time steps, respectively. The analytical sensitivities are computed by utilizing the direct differentiation method (DDM) and the developed AVM, and the numerical one by forward finite difference method (FDM). As shown in Table 2, the agreements between analytical and numerical sensitivities are very good even though the derived adjoint system is a terminal value problem. This is because we saved all the history of responses from original analysis and then performed reverse time integration for the adjoint variables along the saved history.

Table 2 Verification of sensitivity results for various strain-rates

Strain rate	(a) FDM $\Delta\psi/\Delta T$	(b) DDM ψ'_{DDM}	(c) AVM ψ'_{AVM}	(b)/(a) (%)	(c)/(a) (%)
3×10^{10}	−1.4001E+00	−1.4103E+00	−1.4130E+00	100.73	100.92
1.5×10^{10}	−2.0900E+00	−2.1091E+00	−2.1087E+00	100.92	100.90
6×10^{9}	−7.9993E-01	−8.2211E-01	−8.4027E-01	102.77	105.04
3×10^{9}	−2.9399E+00	−2.9151E+00	−3.0615E+00	99.15	104.13

Table 3 Analysis of step size for design perturbation

db	(a) FDM	(b) DDM	(c) AVM	(b)/(a) (%)	(c)/(a) (%)	(c)/(b) (%)
1.00E-10	−1.4300E+00			98.62	98.81	
1.00E-09	−1.4100E+00			100.02	100.21	
1.00E-08	−1.4105E+00			99.99	100.17	
1.00E-07	−1.4103E+00			100.00	100.19	
1.00E-06	−1.2003E+01	−1.4103E+00	−1.4130E+00	11.75	11.77	100.19
1.00E-05	−2.8021E+00			50.33	50.42	
1.00E-04	−9.2028E-01			153.25	153.54	
1.00E-03	−1.6914E+00			83.38	83.54	
1.00E-02	−1.8541E+00			76.06	76.21	

4.1.1 *Accuracy of analytic sensitivity regardless of design perturbation amount*

We analyze the step size of design perturbation to verify the accuracy of the analytical sensitivity obtained from the DDM and the AVM as shown in Table 3. Even though we considered a time-averaged performance measure, when the perturbation amount of temperature is increased, the accuracy of numerical finite difference sensitivity gets extremely decreased since the MD system is highly nonlinear with respect to the design.

4.2 Potential parameter sensitivity on Youngs modulus of nanowires

We utilized an EAM potential to describe the metallic bond between Cu atoms in the numerical examples. In the EAM potential, the total energy of an atom i is given by

$$E_i = F_i\left(\sum_{j\neq i}\rho_j(r_{ij})\right) + \frac{1}{2}\sum_{j\neq i}\phi(r_{ij}), \quad E_{total} = \sum_i E_i, \tag{31}$$

where $F(\rho)$, $\rho(r)$, and $\phi(r)$ denote the embedding energy, local electron density, and pair-wise energy terms, respectively. Usually the three functions in the EAM potential are given as a table of data points that result from fitting to experimental data. Therefore, using the function values, the overall functions within the cut-off distance are extracted by interpolating the data points. To quantify the potential parameter effects on the Youngs modulus of Cu nanowires, we perform the developed adjoint DSA method where the data points for the pair potential function are selected as the design variables. The data points for pair-wise energy term are considered as the design variables as shown in Fig. 4.

4.2.1 *Efficiency of adjoint design sensitivity for many design variables*

The total number of design variables is 500. Note that the developed adjoint variable method needs only one more time integration for the adjoint terminal value problem derived in Eqs. (20)–(24) so that we can obtain design sensitivities with respect to 500 design variables efficiently. However, the required costs for the FDM and the DDM are linearly proportional to the number of design variables. Therefore, we selected arbitrarily four design variables for the FDM to compare with the analytical sensitivities. For example, Fig. 4 shows the design perturbation of 250th design variable. The n-th design variable means the value of data point associate with pairwise potential function as $r_n\phi(r_n)$, where $r_n = n \cdot \Delta r$ and Δr denotes the increment of interatomic distance. The agreement between the finite difference and the adjoint design sensitivities for selected four design variables are listed in Table 4. Even though only four design variables are considered to obtain the finite difference sensitivities, the computational costs for the FDM is linearly proportional to the number of design variables as shown in the Fig. 5. However, the AVM need only about 1.5 times of MD simulations regardless of number of design variables. The efficiency of AVM in the DSA of MD system is already demonstrated in literature where the cost of AVM for 0.25 million design variables is around 1.08 times of cost of MD simulations (Jang et al. 2014).

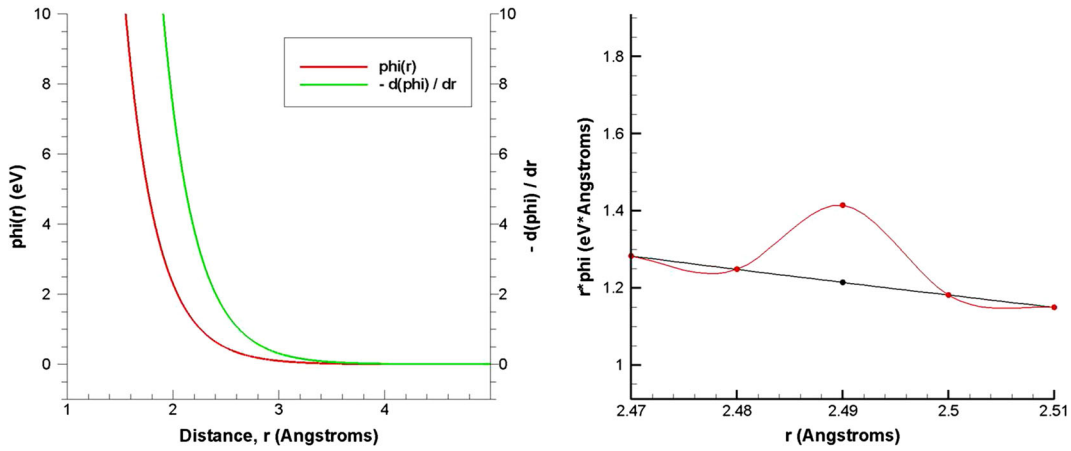

Fig. 4 Interpolated function $\phi(r)$ with its 1st order derivative (*left*) and design perturbation of point value near 2.49 A (*right*). The amount of design perturbations is exaggerated for visualization purpose

Table 4 Sensitivity verification for selected design variables ($\delta b = 10^{-10}$)

D.V.#	(a) FDM	(b) AVM	(b)/(a) (%)
250	−9.17E+02	−9.17E+02	100.00
300	−1.85E+00	−1.85E+00	100.14
350	−3.76E+02	−3.76E+02	99.93
400	−2.66E+01	−2.65E+01	99.92

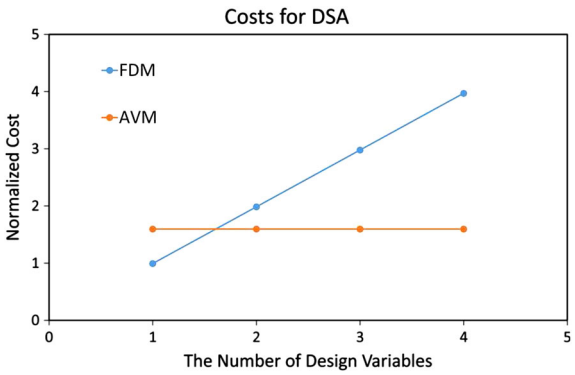

Fig. 5 Comparison of computational costs for FDM and AVM according to the number of design variables

This fact shows that the developed AVM is indispensable to investigate many parameter effects on a performance measure.

5 Conclusions

To quantify the temperature effects on the performance of nanomaterials and gradient of performance measure at a given operation temperature in MD simulations, a DSA method for constant temperature MD is developed. To describe the atomistic behavior of nanomaterials in a desired temperature, the Nose–Hoover thermostat is utilized. The design sensitivity of general performance measures for the constant temperature MD with the Nose–Hoover thermostat is derived using the adjoint variable method since the design problems of MD simulations usually include many design variables. In contrast with the adjoint system of NVE ensemble, that of NVT ensemble cannot be solved from the terminal conditions independently since the MD systems in NVT ensemble are inherently time irreversible. Therefore, the whole time history of responses must be kept in the MD simulation stage for the developed adjoint DSA of the constant temperature MD simulations.The developed adjoint DSA method is applied to a tensile test of Cu Nanowire problem to verify the accuracy and efficiency. The developed adjoint DSA method for constant temperature MD simulations is applicable for the emerging nanotechnology problems such as design of nanomaterials for desired properties and performances.

Acknowledgments This work was supported by the National Research Foundation of Korea (NRF) grant funded by the Korea government (MSIP) (No. 2010-0018282). The authors would also like to thank Ms. Inyoung Cho at Korea University for editing assistance.

Compliance with ethical standards

Conflict of interest The authors declare no conflicts of interest in this work.

References

Adelman, S.A., Doll, J.D.: Generalized langevin equation approach for atom/solid-surface scattering: collinear atom/harmonic chain model. J. Chem. Phys. **61**(10), 4242–4245 (1974). doi:10.1063/1.1681723, http://scitation.aip.org/content/aip/journal/jcp/61/10/10.1063/1.1681723

Adelman, S.A., Doll, J.D.: Generalized langevin equation approach for atom/solid-surface scattering: general formulation for classical scattering off harmonic solids. J. Chem. Phys. **64**(6), 2375–2388 (1976). doi:10.1063/1.432526, http://scitation.aip.org/content/aip/journal/jcp/64/6/10.1063/1.432526

Andersen, H.C.: Molecular dynamics simulations at constant pressure and/or temperature. J. Chem. Phys. **72**(4), 2384–2393 (1980)

Berendsen, H.J., Postma, J.P.M., van Gunsteren, W.F., DiNola, A., Haak, J.: Molecular dynamics with coupling to an external bath. J. Chem. Phys. **81**(8), 3684–3690 (1984)

Ceriotti, M., Bussi, G., Parrinello, M.: Langevin equation with colored noise for constant-temperature molecular dynamics simulations. Phys. Rev. Lett. **102**(2), 020,601 (2009)

Cho, S., Choi, K.K.: Design sensitivity analysis and optimization of non-linear transient dynamics. part i : sizing design. Int. J. Numer. Methods Eng. **48**(3), 351–373 (2000). doi:10.1002/(SICI)1097-0207(20000530)48:3<351:AID-NME878>3.0.CO;2-P

Choi, K., Kim, N.: Structural Sensitivity Analysis and Optimization 2: Nonlinear Systems and Applications. Mechanical Engineering Series, Springer, (2006) http://books.google.co.kr/books?id=zNzUV3PlvycC

Daw, M.S., Foiles, S.M., Baskes, M.I.: The embedded-atom method: a review of theory and applications. Mater. Sci. Rep. **9**(7), 251–310 (1993)

Evstigneev, M., Reimann, P.: Langevin equation for a system nonlinearly coupled to a heat bath. Phys. Rev. B **82**(22), 224,303 (2010)

Frenkel, D., Smit, B.: Understanding Molecular Simulation: From Algorithms to Applications. Computational science series, Elsevier Science, (2001) https://books.google.co.kr/books?id=5qTzldS9ROIC

Hoover, W.G.: Canonical dynamics: equilibrium phase-space distributions. Phys. Rev. A **31**(3), 1695 (1985)

Horstemeyer, M., Baskes, M., Plimpton, S.: Length scale and time scale effects on the plastic flow of fcc metals. Acta Mater. **49**(20), 4363–4374 (2001)

Hsieh, C., Arora, J.: Design sensitivity analysis and optimization of dynamic response. Comput. Methods Appl. Mech. Eng. **43**(2), 195–219 (1984). doi:10.1016/0045-7825(84)90005-7, http://www.sciencedirect.com/science/article/pii/0045782584900057

Hu, Y., Sinnott, S.B.: Constant temperature molecular dynamics simulations of energetic particle-solid collisions: comparison of temperature control methods. J. Comput. Phys. **200**(1), 251–266 (2004)

Jang, H.L., Kim, J.H., Park, Y., Cho, S.: Adjoint design sensitivity analysis of molecular dynamics in parallel computing environment. Int. J. Mech. Mater. Des. **10**(4), 379–394 (2014)

Kim, M.G., Jang, H., Kim, H., Cho, S.: Multiscale adjoint design sensitivity analysis of atomistic-continuum dynamic systems using bridging scale decomposition. Model. Simul. Mater. Sci. Eng. **21**(3), 035005 (2013a), http://stacks.iop.org/0965-0393/21/i=3/a=035005

Kim, M.G., Jang, H.L., Cho, S.: Adjoint design sensitivity analysis of reduced atomic systems using generalized langevin equation for lattice structures. J. Comput. Phys. **240**, 1–19 (2013b). doi:10.1016/j.jcp.2013.01.020, http://www.sciencedirect.com/science/article/pii/S002199911300051X

Koh, S.J.A., Lee, H.P.: Molecular dynamics simulation of size and strain rate dependent mechanical response of fcc metallic nanowires. Nanotechnology **17**(14), 3451 (2006), http://stacks.iop.org/0957-4484/17/i=14/a=018

Lamb, J.S., Roberts, J.A.: Time-reversal symmetry in dynamical systems: a survey. Phys. D Nonlinear Phenom. **112**(1), 1–39 (1998)

Martyna, G.J., Klein, M.L., Tuckerman, M.: Nosé-hoover chains: the canonical ensemble via continuous dynamics. J. Chem. Phys. **97**(4), 2635–2643 (1992)

Nosé, S.: A molecular dynamics method for simulations in the canonical ensemble. Mol. Phys. **52**(2), 255–268 (1984a)

Nosé, S.: A unified formulation of the constant temperature molecular dynamics methods. J. Chem. Phys. **81**(1), 511–519 (1984b)

Shibuta, Y., Suzuki, T.: A molecular dynamics study of the phase transition in bcc metal nanoparticles. J. Chem. Phys. **129**(14), 144102 (2008). doi:10.1063/1.2991435, http://scitation.aip.org/content/aip/journal/jcp/129/14/10.1063/1.2991435

Strogatz, S.H.: Nonlinear Dynamics and Chaos, 1st edn. Perseus Books Group, Cambridge (1994)

Tobias, D.J., Martyna, G.J., Klein, M.L.: Molecular dynamics simulations of a protein in the canonical ensemble. J. Phys. Chem. **97**(49), 12,959–12,966 (1993)

Tsay, J., Arora, J.: Nonlinear structural design sensivitity analysis for path dependent problems. part 1: general theory. Comput. Methods Appl. Mech. Eng. **81**(2), 183–208 (1990)

Tuckerman, M.E., Liu, Y., Ciccotti, G., Martyna, G.J.: Non-hamiltonian molecular dynamics: generalizing hamiltonian phase space principles to non-hamiltonian systems. J. Chem. Phys. **115**(4), 1678–1702 (2001)

Wu, H.: Molecular dynamics study on mechanics of metal nanowire. Mech. Res. Commun. **33**(1), 9–16 (2006)